REVISION

29th November 2014

Pico-Electrochemistry in Humidity-Equilibrated Electrolyte Films on Nano-Cotton: Three- and Four-Point Probe Voltammetry and Impedance

---

Dominic M. Macias [1], Andrew J. Gross [1], Soon Yee Liew,[2] Wim Thielemans [3], John M. Mitchels [1], and Frank Marken *[1]

[1] *Department of Chemistry, University of Bath, Claverton Down, Bath BA2 7AY, UK*
[2] *Process and Environmental Research Division, Faculty of Engineering, The University of Nottingham, Nottingham, NG7 2RD, UK*
[3] *Department of Chemical Engineering, KU Leuven, Campus Kortrijk, Etienne Sabbelaan 53, 8500 Kortrijk, Belgium*

To be submitted to Sensors and Actuators

Proofs to F. Marken (f.marken@bath.ac.uk)

Abstract

Cotton-extracted cellulose nanocrystals are spin-coated from aqueous suspension (0.6 wt%) onto glass slides to give ca. 40 nm thick films. Impregnation with LiCl and redox active $Fe(CN)_6^{3-/4-}$ into this film gives extremely thin redox active layers (typically 170 nm at 60% relative humidity), which were investigated with a 4-point or 3-point probe electrochemical system based on 250 μm diameter platinum wire probes. Both voltammetry and impedance measurements were performed and effects from humidity, concentrations, and time domain on measurements are reported. Only a pico-litre volume under the working electrode was "active" to give a novel electroanalytical "spot test".

Keywords: spot test, cotton, cellulose nanowhiskers, cellulose nanocrystals, electroanalysis, ferrocyanide, sensor.

Graphical Abstract

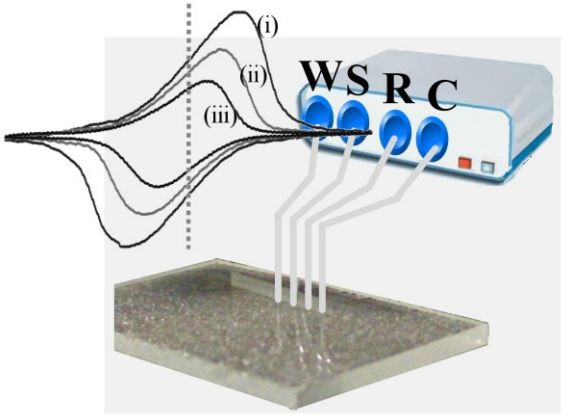

1. Introduction

Small-scale voltammetric analysis is desirable in particular for (i) analysis of expensive (e.g. bio-chemical) redox systems [1], (ii) multi-electrode [2] or high throughput multi-well analysis where thousands of samples need to be screened [3], and (iii) fast response films for example for gas sensing applications [4] where diffusion times need to be minimised. Conventional voltammetric cells operate with typically 10 to 100 cm^3 volume of solvents and in recent work on microfluidic devices this has been reduced to ca. 10^{-9} cm^3 [5]. Here, we aim to reduce this volume by yet another couple of orders of magnitude and propose a method where 10^{-12} cm^{-3} sample volumes could be analysed routinely.

Analysis on cellulose substrates has a long history [6] with many types of pH and spot tests [7,8] as well as chromatography being performed. Paper and cellulose remain popular substrates for new types of electroanalytical methods based on micro-fluidic processes/systems on disposable sensors [9,10]. Nano-cellulose materials have opened up further opportunities in electroanalysis [11] with pure cellulose [12] or composite films [13,14] being readily re-constituted or regenerated, for example on ITO electrode surfaces [15]. Surface-modified nanocrystalline cellulose whiskers have been re-constituted into redox active films with electron transfer occurring between the ferrocene grafts along the nanocrystal surface [16].

Figure 1

Here, a thin film of cotton-extracted nanocrystalline cellulose (ca. 40 nm thickness) is formed via a spin-coating protocol. The glass slide with cellulose nanocrystals and impregnated with a very small volume of electrolyte is shown in Figure 1A. Although almost invisible, the four-point probe measurements clearly reveal the presence of the nanoparticle film and the humidified electrolyte film with redox active components. In order to study the behaviour of the system both 3-point probe (Figure 1B) and 4-point probe (Figure 1C) experiments were performed for the model case of the one-electron $Fe(CN)_6^{3-/4-}$ redox system.

2. Experimental

2.1. Chemical Reagents

LiCl, $K_4Fe(CN)_6$, and $K_3Fe(CN)_6$ were obtained from Sigma-Aldrich or Fisons and used without further purification. Aqueous solutions were prepared using ultrapure water at 20 °C (resistivity ≥ 18.2 MΩ cm).

2.2 Extraction of cellulose nanocrystals from cotton

Nanocrystalline cellulose particles were extracted from pure cotton wool via acid hydrolysis using a 64 wt% aqueous sulfuric acid solution (8.75 ml H_2SO_4 solution per g of cotton) for 40 min at 45 °C under constant stirring. The obtained suspension was centrifuged three times with intermittent washes after quenching the reaction with an equal amount of cold deionized water. The suspension was then dialyzed against tap water to remove residual free acid. A stable dispersion was obtained by sonication (Branson sonifier 250, 10 % amplitude in pulse mode, T < 25 °C) and filtration over a N°2 fritted filter to remove aggregates. Ion exchange resin Amberlite MB 6113 was then added to the dispersion under agitation for 1 hour to protonate the nanocrystal surface and remove non-H^+ ions. The ion exchange resin was removed by filtration followed by another sonication step to individualise the cellulose nanocrystals. The concentration of the final dispersion was determined to be 0.6 wt% by gravimetric analysis.

2.3. Instrumentation and Procedures

Electrochemical measurements were performed at 20 ± 2 °C using an Autolab PGSTAT12 bipotentiostat (Metrohm, UK). A three- or four-electrode configuration was employed with 250 μm diameter platinum wire electrodes with the ends flame-cleaned before use. A Jandel 4-point probe stage was employed initially with standard WC probes (which gave unreliable voltammetry due to more complex electron transfer) and then with platinum wire probes. Relative humidity was measured with a TFA Dostmann/Wertheim sensor. A WS-650Mz-23NPP (Laurell Technologies) spin coater was used to spin the cellulose nanocrystals from a 0.6wt% aqueous suspension onto glass slides (prepared from

microscopy slides). Scanning electron microscopy (SEM) images were obtained after 5 nm chromium coating with a JSM-6480LV (JEOL, Japan) and analysed using imageJ 1.48v software. Atomic Force Microscopy (AFM) images were obtained using a Digital Instruments Nanoscope IIIa Multimode Scanning Probe Microscope in tapping mode (Veeco TESP probes).

2.4. Film Formation

A solution of 0.6wt% of nano-cotton in water was spin-coated onto a glass slide (cleaned by heat treatment for 30 minutes at 450 ^{o}C) to obtain the nano-cotton film. Five coatings were applied by spinning at 500 rpm (15 s) then 3000 rpm (30s) per coating. Electron microscopy (Figure 2A) and atomic force microscopy (Figure 2B and 2C) images confirm a uniform deposit with a typical thickness (see cross-section in Figure 2C) of 40 nm.

Figure 2

An electrolyte solution containing 0.1 M LiCl and 1 mM $K_4Fe(CN)_6$ and 1 mM $K_3Fe(CN)_6$ (unless stated otherwise) in water is then deposited evenly on the cotton-modified glass slide (1 μL on 1 cm^2) and the sample is placed in an oven to equilibrate for 60 minutes at 100 ^{o}C. Once removed from the oven, the sample was re-equilibrated in air (or under controlled humidity) for 60 minutes before performing electrochemical experiments. The

equilibrium concentration of LiCl is relative humidity (RH) dependent as described by the approximate relationship given in Equation 1 (derived from reference [17]; note an error in this reference where values for constants A and B in table 1 are exchanged; LiCl solution density values obtained from [18]). For a range of relative humidities from 40% to 80% the equilibrium concentration of LiCl (in mol dm^{-3}) in water is predicted to range from 8.0 to 4.5 mol dm^{-3}. This corresponds to an electrolyte solution volume decrease of 80 to 45 times, respectively.

$$RH(in\ \%) = 100 \times \exp\left(0.675 - 0.198 \times c_{LiCl}\right) \quad (1)$$

3. Results and Discussion

Initially, 3-point probe voltammetry experiments were performed with a deposit of 0.1 M LiCl and 1 mM $K_4Fe(CN)_6$ and 1 mM $K_3Fe(CN)_6$ in the cotton-derived cellulose nanocrystal film. As a result of the atmospheric relative humidity, this solution will equilibrate to a lower volume. Typically, experiments were performed at 60% relative humidity, which based on Equation 1 leads to an approximate LiCl concentration of 6 M or a 60-fold decrease in solution volume. Accordingly, the redox system is 60 mM $K_4Fe(CN)_6$ and 60 mM $K_3Fe(CN)_6$.

Figure 3

Figure 3 shows typical cyclic voltammetry data for the $Fe(CN)_6^{3-/4-}$ redox system with the electrochemically reversible oxidation/reduction clearly visible (see Equation 2). The voltammetric signal is centred at E_{mid} = ½ $E_{p,ox}$ + ½ $E_{p,red}$ = 0.0 V due to the platinum pseudo-reference electrode being placed into the same $Fe(CN)_6^{3-/4-}$ redox solution.

$$Fe(CN)_6^{3-}\,(aq) + e^- \rightleftharpoons Fe(CN)_6^{4-}\,(aq) \qquad (2)$$

When adjusting the relative humidity (by adding a humid nitrogen flow into a Perspex containment) from 60% to 80%, the voltammetric signal is affected only insignificantly. Generally, the voltammetric response increases with humidity, which may be attributed to two effects: (i) the volume of solution is increased and thereby more $Fe(CN)_6^{3-/4-}$ is accessible and (ii) the resistance component in the voltammetric signals (*vide infra*) is lowered and therefore the peak current increased. Overall, the effect of humidity seemed less important and therefore the remaining measurements were performed at ambient ca. 60% relative humidity.

Repeat measurements at different points on the sample revealed some variability (+/- 50%), which is likely to be caused either by thickness variations in the deposited cellulose nanocrystal film or variation in surface tension (*vide infra*). Voltammetric peak responses show no pronounced diffusional "tail" as is observed for conventional diffusion-controlled behaviour. The observed peak responses are therefore associated with a local "confined"

diffusion space possibly underneath the working electrode probe. When changing the scan rate, the charge under the voltammetric signal remains relatively constant (see Figure 3B and 3C) with only a slight decrease observed at higher scan rates. The charge under the peak is typically 3.6 μC, which suggests a 37 pmol redox active component, or an active volume of 310 pL. This suggests an "active spot" on the nanocrystal film with ca. 500 μm radius which compares to the platinum wire radius of 125 μm. Most likely, a meniscus of active solution is present surrounding the working electrode (see Figure 3D).

Figure 4 shows 3-point probe voltammetry for samples with varying concentration of $Fe(CN)_6^{3-}$ and $Fe(CN)_6^{4-}$. Similarly clear voltammetric features are observed at lower concentrations, but the reference potential is less stable and therefore a shift of the signal is seen. Perhaps surprisingly, the charge under the oxidation or reduction peak responses does not scale linearly with the concentration of the redox reagent, which may be indicative of a more complex system including adsorption to the nanocrystal surfaces or precipitation phenomena.

Figure 4

Interesting is also the apparent increase in the resistivity that causes the widening of the peak-to-peak separation in the voltammetric response. For an ideal voltammetric response with contributions from diffusion the peak-to-peak separation should be 0 Volt. It is therefore possible to estimate the average resistivity from the increase in peak-to-peak separation based on equation 3:

$$R = \frac{E_{p,ox} - E_{p,red}}{I_{p,ox} - I_{p,red}} \quad (3)$$

For the three cases in Figure 4 the estimated resistance values are obtained as (i) 0.18 MΩ, (ii) 1.2 MΩ, and (iii) 2.4 MΩ for 1 mM, 0.1 mM, and 0.01 mM $Fe(CN)_6^{3-/4-}$, respectively. These apparent resistance values are caused by the current flow and the resulting potential gradient over the nanocellulose film with respect to the position of the reference probe. The resistance is likely to be unevenly distributed over the working electrode surface (reaching into the meniscus) with regions closer to the counter electrode experiencing higher resistance. A better approach for the determination of the "true" resistivity in the thin electrolyte film can be based on 4-point probe measurements (see Figure 4D) where the inner two probes (see Figure 1C) operate as a potential gradient sensor (with the help of the reversible $Fe(CN)_6^{3-/4-}$ redox probe). With a relatively large potential window of 0.5 V reasonably linear (Ohmic) current responses are observed which suggest resistance values of (i) 60 kΩ, (ii) 0.6 MΩ, and (iii) 1.2 MΩ for 1 mM, 0.1 mM, and 0.01 mM $Fe(CN)_6^{3-/4-}$, respectively. However, more precise measurements are possible with less polarisation and with a smaller potential amplitude and employing impedance methods. The nature of this resistivity effect requires more study, but when confirmed for other types of analyte, this parameter could be employed analytically.

Figure 5

Four-point probe impedance measurements (see Figure 5A) confirm the presence of an Ohmic resistance within the electrolyte film of ca. 64 kΩ consistent with the 4-point probe voltammetry measurement. At frequencies higher than 200 Hz artefacts due to the 4-point probe geometry and sample properties are observed (e.g. inductive behaviour due to the non-ideal geometry [19]). Nevertheless, within the chosen measurement range phase angle and Bode impedance plots confirm resistive behaviour.

Figure 5B shows impedance data for the 3-point probe measurement configuration where the Faradaic current responses also show significant effects. The resulting RC element shows a resistance of ca. 100 kΩ at higher frequencies and then an increasing capacitive component towards lower frequencies consistent with the presence of the $Fe(CN)_6^{3-/4-}$ redox system and absence of diffusional transport. Both types of measurement geometries, 3-point and 4-point probe, and both types of measurement modes, voltammetry and impedance, could be of use in thin film sensor or chromatography applications [20]. In future, in particular the use of a wider range of chemically selective/responsive redox systems could provide very fast and versatile sensor systems.

4. Conclusion

For the model redox system $Fe(CN)_6^{3-/4-}$ in aqueous electrolyte solution, it has been shown that thin film voltammetry and impedance measurements are possible on a cellulose nanocrystal substrate and with extremely thin layers of electrolyte (ca. 100 nm). The impedance measurement offers high sensitivity with potential for future development into gas or humidity detection systems. In contrast, the voltammetry experiment offers a new approach to microphase redox cycling [21] where the redox reagent can become an active ingredient of the sensor process [22]. This could be developed for example into H_2S selectivity [23] or biological oxygen demand detection [24] and many other chemically selective electroanalytical processes. By operating in a very small (310 pL or less) volume, this technique could become very fast (no diffusional delays) and able to deal with arrays of samples, for example in high-throughput applications. Improvements for future pico-electroanalytical sensor applications will be necessary in particular in (i) the nanocellulose substrate, (ii) the design of the probe electrodes (shape, diameter, positioning), and (iii) in the choice of electrolyte system (concentration and type of humidity-responsive electrolyte).

Acknowledgements

A.J.G. and F.M. gratefully acknowledge the Engineering and Physical Sciences Research Council (EP/I028706/1) for financial support. W.T. thanks the Fonds Wetenschappelijk Onderzoek (FWO, grant G.0C60.13N) for financial support.

References

[1] G. Wittstock, T. Wilhelm, S. Bahrs, P. Steinrücke, SECM feedback imaging of enzymatic activity on agglomerated microbeads, Electroanalysis, 13 (2001) 669-675.

[2] F. Tan, J.P. Metters, C.E. Banks, Electroanalytical applications of screen printed microelectrode arrays, Sens Actuators, B, 181 (2013) 454-462.

[3] T. Erichsen, S. Reiter, V. Ryabova, E.M. Bonsen, W. Schuhmann, W. Märkle, C. Tittel, G. Jung, B. Speiser, Combinatorial microelectrochemistry: Development and evaluation of an electrochemical robotic system, Rev Sci Instrum, 76 (2005) 062204.

[4] E.I. Rogers, A.M. O'Mahony, L. Aldous, R.G. Compton, Amperometric gas detection using room temperature ionic liquid solvents, ECS Trans, 7 ed. 2010, pp. 473-502.

[5] G. Bontempelli, N. Comisso, R. Toniolo, G. Schiavon, Electroanalytical sensors for nonconducting media based on electrodes supported on perfluorinated ion-exchange membranes, Electroanalysis, 9 (1997) 433-443.

[6] I. Smith, J.G. Feinberg, Chromatography and electrophoresis on paper: A teaching level manual: Pergamon Press, London; 1962.

[7] F. Feigl, Spot Tests in Organic Analysis: Elsevier Publishing Company, Amsterdam: 1960.

[8] F. Feigl, Organic spot test analysis, Anal Chim Acta, 27 (1955) 1315-1318.

[9] W.-J. Lan, E.J. Maxwell, C. Parolo, D.K. Bwambok, A.B. Subramaniam, G.M. Whitesides, Paper-based electroanalytical devices with an integrated, stable reference electrode, Lab Chip, 13 (2013) 4103-4108.

[10] J. Lankelma, Z. Nie, E. Carrilho, G.M. Whitesides, Paper-based analytical device for electrochemical flow-injection analysis of glucose in urine, Anal Chem, 84 (2012) 4147-4152.

[11] S.Y. Liew, S. Shariki, A. Vuorema, D. A. Walsh, F. Marken, W. Thielemans, Cellulose nanowhiskers in electrochemical applications, in: F. Liebner, T. Rosenau (Eds.), Functional Materials from Renewable Sources, American Chemical Society 2012, pp. 75-106.

[12] S. Shariki, S.E.C. Dale, F. Marken, Electroanalysis at Salt - Cotton - Electrode Interfaces: Preconcentration Effects Lead to Nano-Molar Hg^{2+} Sensitivity. Electroanalysis, 23 (2011) 2149-2155.

[13] M.J. Bonné, E. Galbraith, T.D. James, M.J. Wasbrough, K.J. Edler, A.T.A. Jenkins, et al., Boronic acid dendrimer receptor modified nanofibrillar cellulose membranes, J Mater Chem, 20 (2010) 588-594.

[14] M.J. Bonné, K.J. Edler, J.G. Buchanan, D. Wolverson, E. Psillakis, M. Helton, F. Marken, Thin-film modified electrodes with reconstituted cellulose-PDDAC films for the accumulation and detection of triclosan, J Phys Chem C, 112 (2008) 2660-2666.

[15] A. Vuorema, M. Sillanpää, M. Vehviläinen, T. Kamppuri, P. Nousiainen, W. Thielemans, F. Marken, Self-assembled regenerated cellulose spacer film in thin film and generator-collector electrodes, Electroanalysis, 25 (2013) 1773-1779.

[16] S. Eyley, S. Shariki, S.E.C. Dale, S. Bending, F. Marken, W. Thielemans, Ferrocene-decorated nanocrystalline cellulose with charge carrier mobility, Langmuir, 28 (2012) 6514-6519.

[17] S.I. Prokopiev, Y.I. Aristov, Concentrated aqueous electrolyte solutions: Analytical equations for humidity - concentration dependence, J Solution Chem, 29 (2000) 633-649.

[18] I.M. Abdulagatov, N.D. Azizov, Densities and apparent molar volumes of concentrated aqueous LiCl solutions at high temperatures and high pressures, Chem Geol, 230 (2006) 22-41.

[19] S. Fletcher, The two-terminal equivalent network of a three-terminal electrochemical cell, Electrochem Commun, 3 (2001) 692-696.

[20] M.R. Gama, C.H. Collins, C.B.G. Bottoli, Nano-liquid chromatography in pharmaceutical and biomedical research, J Chromatogr Sci, 51 (2013) 694-703.

[21] S.E.C. Dale, C.Y. Cummings, F. Marken, Microphase Salt matrix voltammetry: Microphase redox processes at ammonium chloride | gold | gas triple phase boundaries. Electrochem. Commun., 13 (2011) 154-157.

[22] J.H. Zagal, S. Griveau, J.F. Silva, T. Nyokong, F. Bedioui, Metallophthalocyanine-based molecular materials as catalysts for electrochemical reactions, Coord Chem Rev, 254 (2010) 2755-2791.

[23] B. Spilker, J. Randhahn, H. Grabow, H. Beikirch, P. Jeroschewski, New electrochemical sensor for the detection of hydrogen sulfide and other redox active species, J Electroanal Chem, 612 (2008) 121-130.

[24] H. Chen, T. Ye, B. Qiu, G. Chen, X. Chen, A novel approach based on ferricyanide-mediator immobilized in an ion-exchangeable biosensing film for the determination of biochemical oxygen demand, Anal Chim Acta, 612 (2008) 75-82.

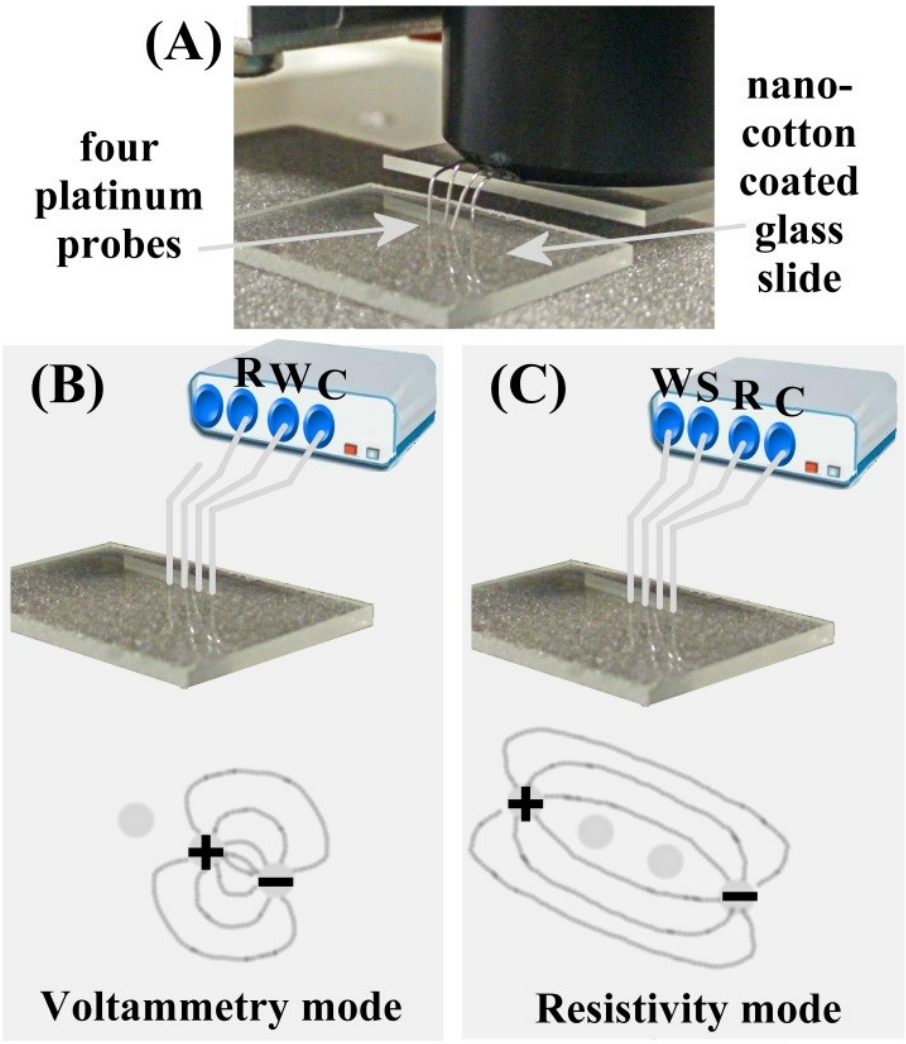

Figure 1. (A) Photograph of the 4-point probe with 250 μm diameter platinum wires with approximately 1 mm inter-electrode gap positioned on a cotton-extracted nanocrystalline cellulose modified glass slide. (B) Schematic drawing of the 3-point probe configuration for voltammetry. (C) Schematic drawing of the 4-point probe configuration for resistance measurements.

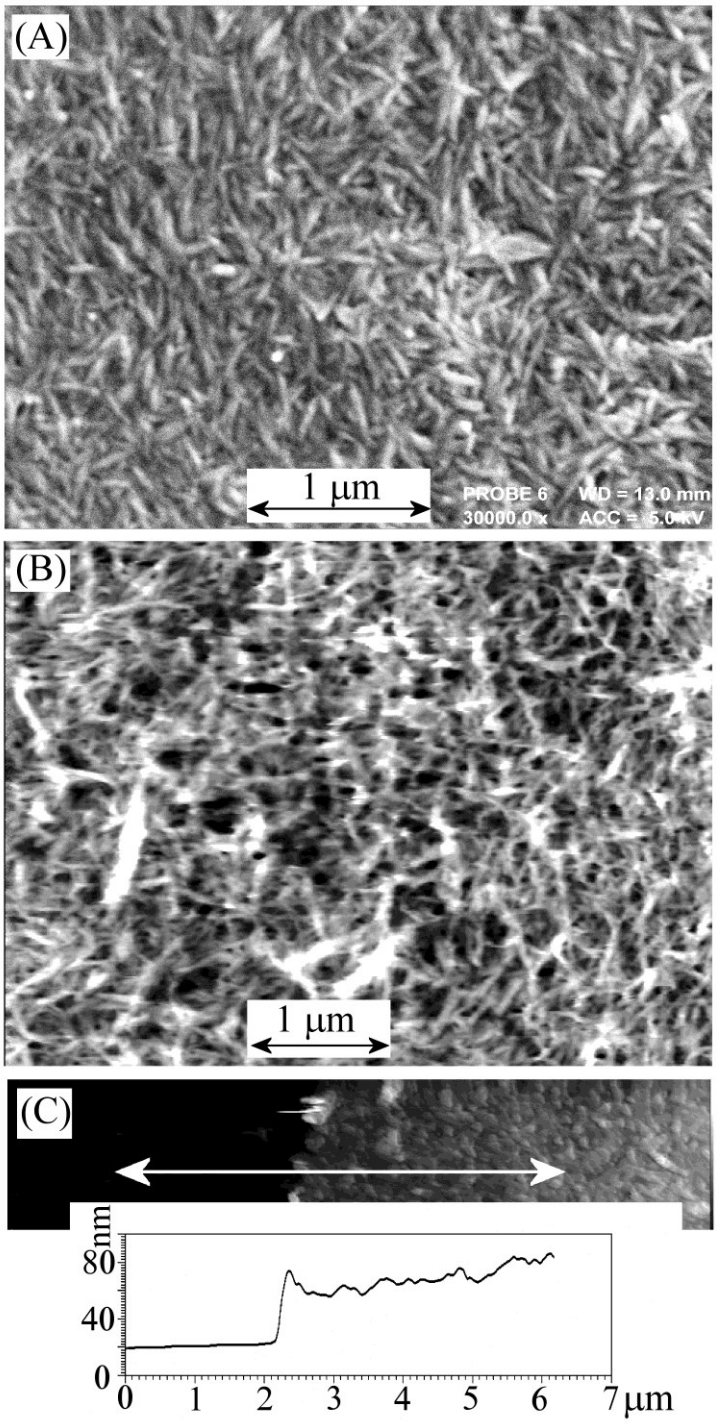

Figure 2. (A) Scanning electron microscopy (SEM; with 5 nm chromium layer to promote conductivity) and (B) atomic force microscopy (AFM) images of nanocrystalline cellulose spin-coated onto glass. (C) AFM cross-sectional image showing typical thickness of 40 nm.

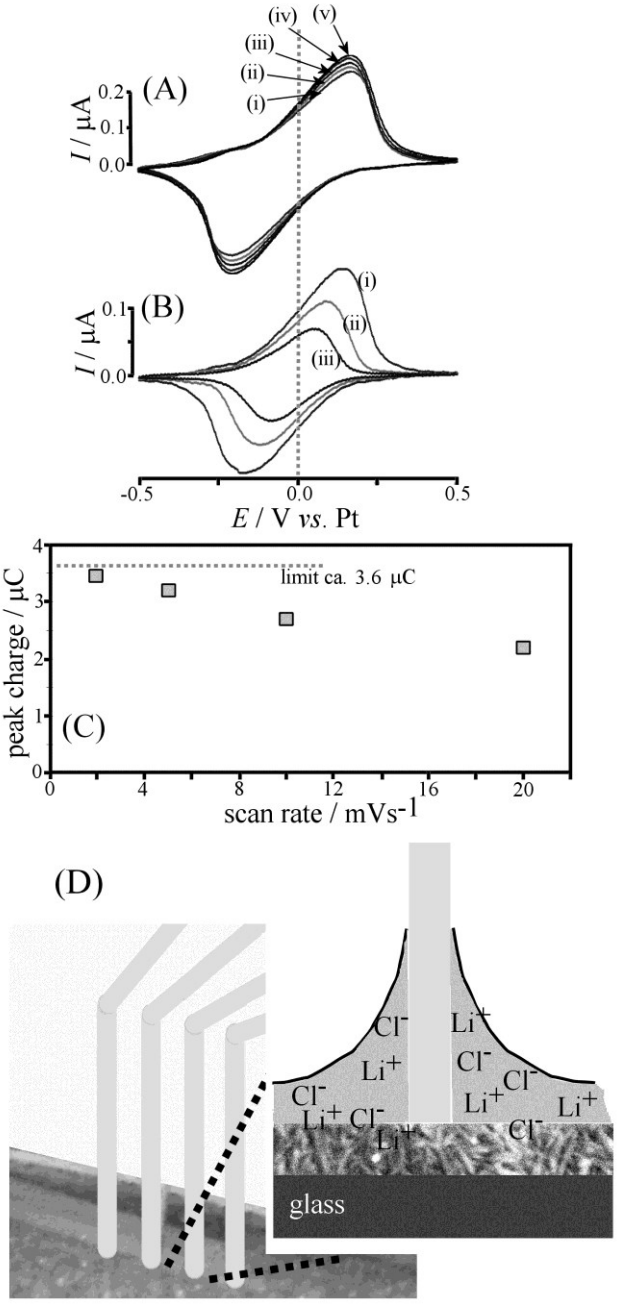

Figure 3. (A) Cyclic voltammograms (scan rate 20 mVs^{-1}) for a film formed from 0.1 M LiCl and 1 mM $K_4Fe(CN)_6$ and 1 mM $K_3Fe(CN)_6$ in a cellulose nanocrystal film in an atmosphere with (i) 60%, (ii) 65%, (iii) 70%, (iv) 75%, (v) 80% relative humidity. (B) Cyclic voltammograms (scan rate (i) 20, (ii) 10, and (iii) 5 mVs^{-1}) at 60% relative humidity. (C) Plot of the charge under the voltammetric peak *versus* scan rate. (D) Schematic drawing of the electrode sample contact (not to scale).

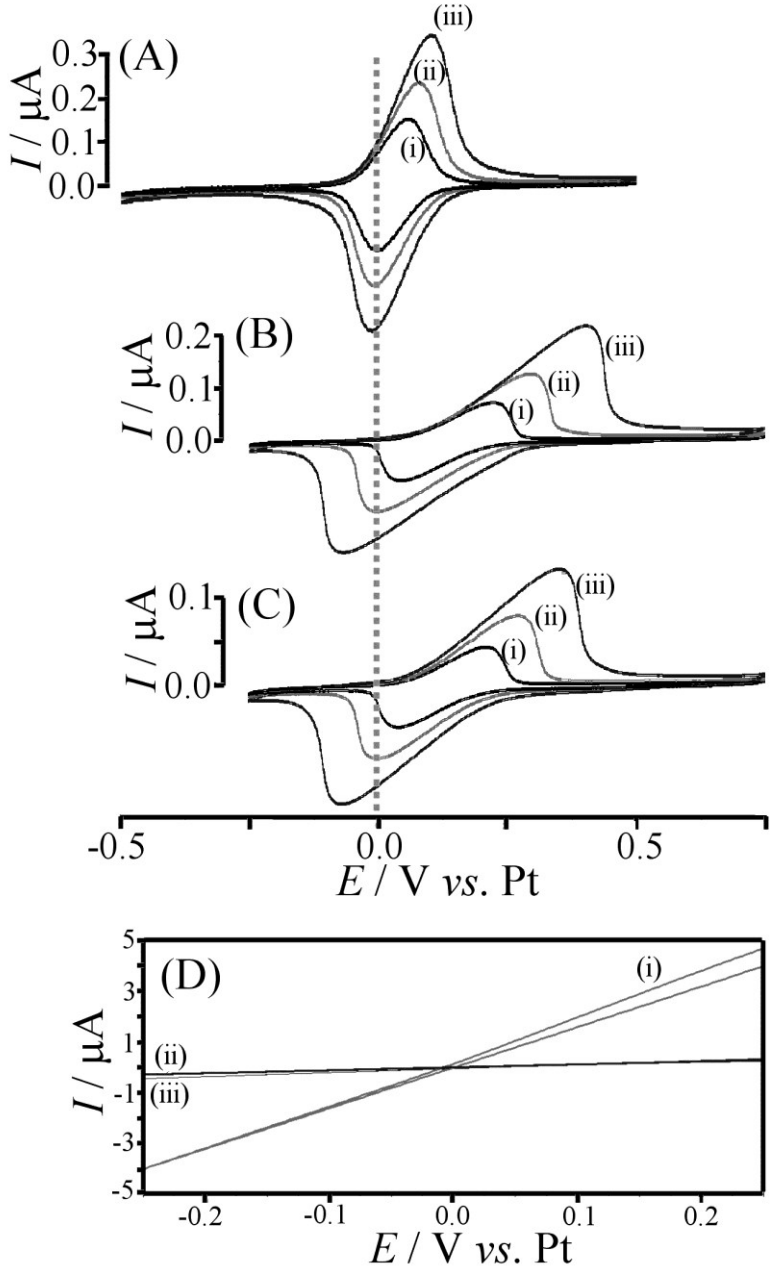

Figure 4. (A) Cyclic voltammograms (scan rate (i) 5, (ii) 10, (iii) 20 mVs^{-1}) for a film formed from 0.1 M LiCl and 1 mM $K_4Fe(CN)_6$ and 1 mM $K_3Fe(CN)_6$ in a cellulose nanocrystal film in an atmosphere with 60% relative humidity. (B) As above but with 0.1 mM $K_4Fe(CN)_6$ and 0.1 mM $K_3Fe(CN)_6$. (C) As above but with 0.01 mM $K_4Fe(CN)_6$ and 0.01 mM $K_3Fe(CN)_6$. (D) Four-point probe voltammetry measurement (scan rate 10 mVs^{-1}) of resistance responses for the above three samples with (i) 1 mM $K_4Fe(CN)_6$ and 1 mM $K_3Fe(CN)_6$, (ii) 0.1 mM $K_4Fe(CN)_6$ and 0.1 mM $K_3Fe(CN)_6$, and (iii) 0.01 mM $K_4Fe(CN)_6$ and 0.01 mM $K_3Fe(CN)_6$.

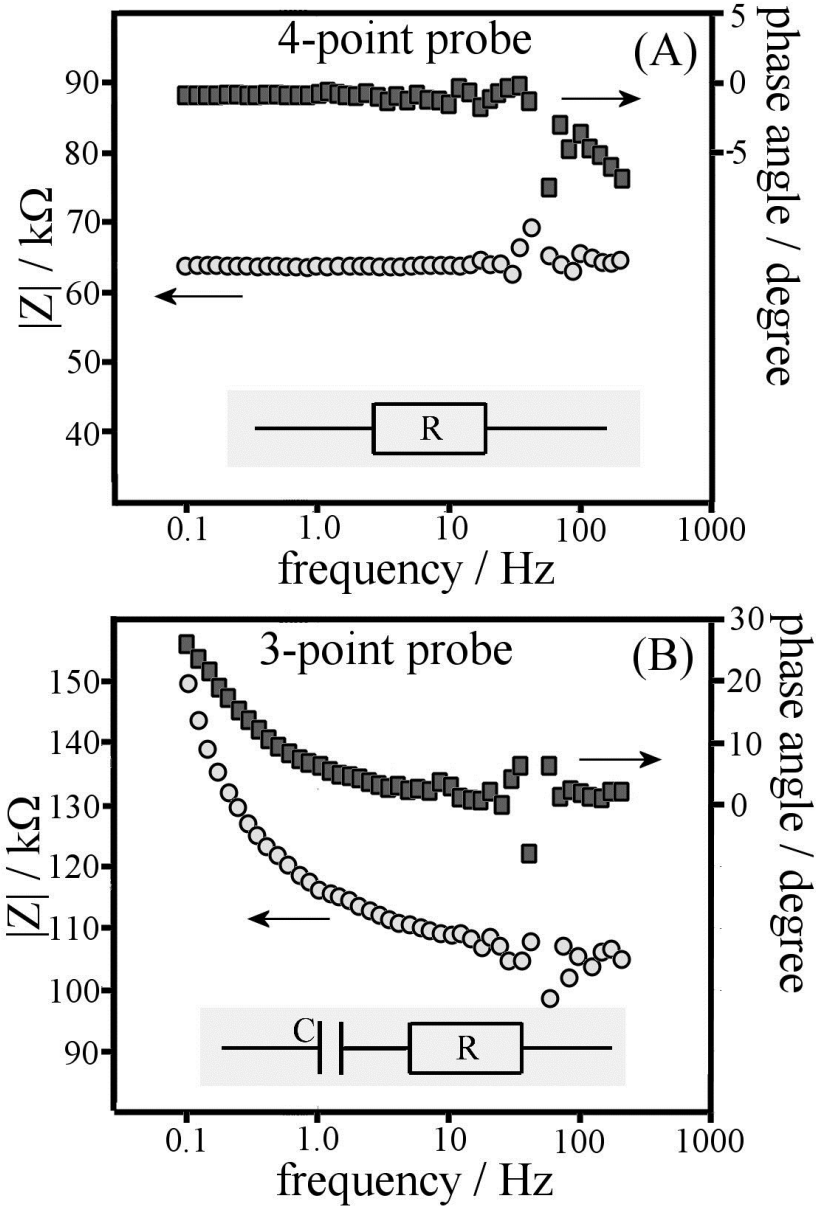

Figure 5. Bode plots for (A) 4-point probe and (B) 3-point-probe impedance data (frequency range 200 to 0.1 Hz, amplitude 25 mV, at open circuit potential) for a film formed from 0.1 M LiCl and 1 mM $K_4Fe(CN)_6$ and 1 mM $K_3Fe(CN)_6$ in a nanocrystalline cellulose film in an atmosphere with 60% relative humidity.